Analysis of the energy exchange between coupled subsystems by means of the divergence in the vibratory energy field

Peter Groba[1], Johannes Ebert[1], Torsten Stoewer[1], Joachim Bös[2] und Tobias Melz[2]
[1] *BMW Group, 80788 München, Deutschland, Email: peter.groba@bmw.de*
[2] *TU Darmstadt, Fachgebiet SAM, 64289 Darmstadt, Deutschland*

Introduction

One way of analysing a system with respect to its acoustical properties is to take a look at energetic phenomena and behaviours. A method widely used is the description of the energy flow in terms of acoustic intensities in both the structure and the fluid. With this approach, a link between the excitation and the radiation is created. In order to get a more holistic view on the acoustical chain of effects, this paper and the related work aims for a better understanding of the mechanisms that link different subsystems. This is done by analysing the energy transfer over system boundaries. In this paper, the equations are derived to quantify the exchange of structure-based vibratory energy and the first numerical calculation results are shown for a simple test case.

Describing vibratory energy and power

The structural intensity (STI) is a widely used quantity in acoustical analysis. For three dimensional structures in steady-state, the cross-spectral density of the complex stress tensor, $\underline{\mathbf{S}}$, and the conjugate of the complex velocity vector, $\underline{\mathbf{v}}^*$, yields the complex STI [1]

$$\underline{\mathbf{I}}_\mathrm{s}(f) = -\frac{1}{2}\underline{\mathbf{S}}(f) \cdot \underline{\mathbf{v}}^*(f) \tag{1}$$

in the frequency domain. This paper focuses on thin-walled structures for which the KIRCHHOFF plate theory applies. The complex STI in plate and more general shell elements, $\underline{\mathbf{I}}'(f)$, is calculated by means of section forces and moments and their multiplication with the respective translational and rotational velocities [1]

$$\underline{\mathbf{I}}'(f) = -\frac{1}{2}\begin{bmatrix} \underline{N}_x\underline{v}_x^* + \underline{N}_{xy}\underline{v}_y^* + \underline{M}_x\underline{\dot{\varphi}}_y^* - \underline{M}_{xy}\underline{\dot{\varphi}}_x^* + \underline{Q}_x\underline{v}_z^* \\ \underline{N}_y\underline{v}_y^* + \underline{N}_{yx}\underline{v}_x^* - \underline{M}_y\underline{\dot{\varphi}}_x^* + \underline{M}_{yx}\underline{\dot{\varphi}}_y^* + \underline{Q}_y\underline{v}_z^* \end{bmatrix}. \tag{2}$$

The connection between Equation (1) and (2) is given through the integration of the STI in the z-direction

$$\underline{\mathbf{I}}'(f) = \int_{-\frac{h}{2}}^{\frac{h}{2}} \underline{\mathbf{I}}_\mathrm{s}(f)\ \mathrm{d}z. \tag{3}$$

This yields the energy flow over the thickness, h, of the plate. A simplification is made for thin-walled structures. The energy flow in the z-direction is considered small in comparison to the components in x- and y-directions and is therefore neglected. This leads to the two dimensional problem in Equation (2).

The descriptions in this paper refer to the active energy flow. The active part of the complex intensity, in the frequency domain,

$$\mathbf{I}_\mathrm{s,a}(f) = \mathrm{Re}\left(\underline{\mathbf{I}}_\mathrm{s}(f)\right) = \lim_{T\to\infty}\frac{1}{T}\int_{t=0}^{T}\mathbf{I}_\mathrm{s}(t)\mathrm{d}t \tag{4}$$

is related to the time-averaged value of the STI in the time domain, $\mathbf{I}_\mathrm{s}(t)$, [1]. For reasons of simplicity in the following explanations, if not explicitly stated, the equations always relate to the real part of the STI.

In order to gain additional information about the analysed energy field, the STI's divergence, $\mathrm{div}(\mathbf{I}_\mathrm{s})$, is calculated through scalar multiplication of the nabla operator, ∇, with the STI vector

$$\mathrm{div}(\mathbf{I}_\mathrm{s}) = \nabla \cdot \mathbf{I}_\mathrm{s} = \frac{\partial}{\partial x_i}I_i = \frac{\partial I_x}{\partial x} + \frac{\partial I_y}{\partial y} + \frac{\partial I_z}{\partial z}. \tag{5}$$

In general, the divergence allows for the identification of sources and sinks in the considered vector field. Figure 1 shows the calculation result of the STI's divergence for the fourth natural frequency of a simply supported rectangular aluminium plate under harmonic force excitation. The plate possesses a length of 860 mm, a width of 630 mm, and a thickness of 4 mm. The color scale of the STI's divergence is superimposed with the STI vector field to depict the direction of the energy flow. The values greater than zero marked in red in the lower left area of the plate correctly identify the point of the force excitation. The three areas with increased negative divergence values are indicating areas with higher energy dissipation in the plate. The mode shape in the depicted case is the 3-1-mode. Figure 1 shows that for the example of the rectangular plate the areas of high energy dissipation correspond to the mode shape of the excitation frequency.

In this state, it is possible to identify areas with positive and negative values of the STI's divergence and to give predictions for the locations of energy sources and sinks in the vibratory energy field. A question that remains is, can reliable information about the quantity of the energy input and output be derived from the absolute values of the divergence? In order to give an answer to this question, the divergence of the STI is considered in

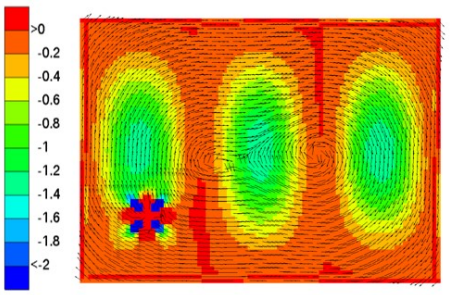

Figure 1: The STI's divergence, in Wm^{-2}, for the fourth natural frequency of a simply supported rectangular plate (color scale) and the corresponding direction of the energy flow (arrows)

the context of energy exchanges in a closed system as described by the first law of thermodynamics. The change of the energy density, e, over time is connected to the STI, the input, π_{in}, and the dissipated energy density, π_{diss}, in a control volume [2]

$$\iiint_V \frac{\partial e(t)}{\partial t}\mathrm{d}V = -\iint_{A_\mathrm{s}} \mathbf{I}_\mathrm{s}(t)\mathbf{n}_\mathrm{s}\mathrm{d}A + \iiint_V (\pi_{\mathrm{in}} - \pi_{\mathrm{diss}})\mathrm{d}V. \tag{6}$$

In case of a steady-state, the left side of Equation (6) becomes zero as there is no change of the average energy density [1]. The STI's term is written on the left side and the energy densities are integrated over the volume, V. This yields the following relationship for the frequency domain

$$\iint_{A_\mathrm{s}} \mathbf{I}_\mathrm{s}(f)\mathbf{n}_\mathrm{s}\mathrm{d}A = P_{\mathrm{s,in}}(f) - P_{\mathrm{s,diss}}(f). \tag{7}$$

This paper discusses the STI and its divergence for thin-walled structures. The aim is to use these values to derive power balance equations. By using the divergence theorem

$$\iiint_V \mathrm{div}(\mathbf{I}_\mathrm{s}(f))\mathrm{d}V = \iint_{A_\mathrm{s}} \mathbf{I}_\mathrm{s}(f)\mathbf{n}_\mathrm{s}\mathrm{d}A \tag{8}$$

the integral of the STI over the area, A, is transformed into an integral over the volume, V. Furthermore, since the integration boundaries in the volume integral in Equation (8) are independent from each other, it is possible to calculate them separately

$$\iiint_V \mathrm{div}(\mathbf{I}_\mathrm{s}(f))\mathrm{d}V = \int_0^{l_x}\int_0^{l_y}\int_{-\frac{h}{2}}^{\frac{h}{2}} \mathrm{div}(\mathbf{I}_\mathrm{s}(f))\mathrm{d}z\mathrm{d}y\mathrm{d}x. \tag{9}$$

The divergence of the STI is gained through summation of the partial derivatives. Inserting Equation (5) in Equation (9) and omitting the component in the z-direction yields

$$\iiint_V \mathrm{div}(\mathbf{I}_\mathrm{s}(f))\mathrm{d}V = \int_0^{l_x}\int_0^{l_y}\int_{-\frac{h}{2}}^{\frac{h}{2}} \left(\frac{\partial I_x}{\partial x} + \frac{\partial I_y}{\partial y}\right)\mathrm{d}z\mathrm{d}y\mathrm{d}x. \tag{10}$$

Since the remaining intensity terms in the sum are now independent from z and the integration over the thickness of the plate has fixed boundaries it is possible to change the succession of the mathematical operations. After conducting the integration over the thickness

$$\iiint_V \mathrm{div}(\mathbf{I}_\mathrm{s}(f))\mathrm{d}V = \int_0^{l_x}\int_0^{l_y} \left(\frac{\partial I'_x}{\partial x} + \frac{\partial I'_y}{\partial y}\right)\mathrm{d}y\mathrm{d}x \tag{11}$$

it is possible to rewrite the sum of the terms $\frac{\partial I'_x}{\partial x}$ and $\frac{\partial I'_y}{\partial y}$ as $\mathrm{div}(\mathbf{I}'(f))$. It can now be seen that the volume integral of the STI's divergence, in this special case, equals the integral over the surface area for the divergence in shells

$$\iiint_V \mathrm{div}(\mathbf{I}_\mathrm{s}(f))\mathrm{d}V = \iint_{A_\mathrm{s}} \mathrm{div}(\mathbf{I}'(f))\mathrm{d}A. \tag{12}$$

This leads to an equation where the divergence of the STI in thin-walled structures is related to the power input and the dissipated power in a specific area of the structure

$$\iint_{A_\mathrm{s}} \mathrm{div}(\mathbf{I}'(f))\,\mathrm{d}\,A = P_{\mathrm{s,in}}(f) - P_{\mathrm{s,diss}}(f). \tag{13}$$

Introducing artificial system boundaries

The description of energy exchange is enabled by means of a simplified approach. As shown in Figure 2, two calculations are conducted on the basis of the same STI values. The first calculation, in the left path, is conducted on the original STI vector field. The right path depicts that in order to simulate an energy transfer in a simple test structure an intermediate step is added. In this step, the STI in the artificial connection area is set to zero before calculating the divergence. With this, auxiliary system boundaries are created in the structure [3].

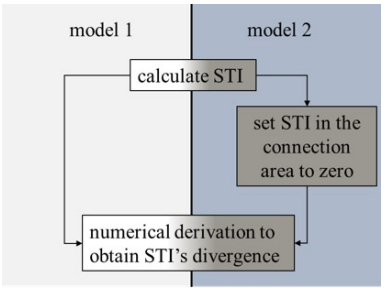

Figure 2: Scheme of the calculation approach [3]

The test structure is the rectangular plate already used for the calculation shown in Figure 1. Figure 3 depicts the calculation result for the outlined approach at the same natural frequency as before. The energy barrier is simulated through setting the energy flow to zero in a small band in the middle of the plate. In this example, the energy diverges from the excitation in the lower left corner of the plate and creates a clockwise energy flow. At the auxiliary boundary to the artificial connection the

divergence shows increased values in contrast to the adjacent areas. In the upper half of the left boundary the divergence shows negative values. This indicates an energy sink for the excited area of the plate, which is in accordance with the direction of the energy vectors that flow from the excited area into the connection area. Following the energy path, the vectors enter the right side of the structure. In this case, the divergence shows positive values and thus indicates an energy source. At the connection the divergence shows both positive and negative values at each side of the connection. This is due to the energy that flows back from the right to the left side of the structure.

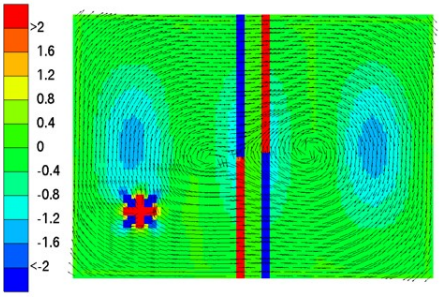

Figure 3: The STI's divergence, in Wm^{-2} (color scale), for the fourth natural frequency of a simply supported rectangular plate in case of the simulation of an artificial connection area

Power balance in systems

This section addresses the significance of the values obtained through calculation of the STI's divergence. To evaluate this, the divergence is linked to power values.

The first check of the result of the numerical derivation is conducted by calculating the overall power balance of the structure. In a steady-state, the introduced system is in balance between the input power and the power that is dissipated by the structure. In this balanced state, $P_{\mathrm{s,in}}(f)$ should equal $P_{\mathrm{s,diss}}(f)$ and according to Equation (13) the integral of the STI over the whole structure then must be equal to zero. The outcome of this calculation is shown in Figure 4. The overall power, P_{div}, is in accordance with the stated assumption. The value slightly differs from zero, but in a negligible order. The overall value is set in contrast to the input power of the force excitation calculated through multiplication of the complex forces and velocities

$$P_{\mathrm{in}}(f) = -\frac{1}{2}\,\mathrm{Re}\left(\underline{\mathbf{F}}(f)\cdot\underline{\mathbf{v}}^{*}(f)\right). \qquad (14)$$

A comparison of the input power and the overall power balance results in an error that is below 1%.

The satisfactory result, considering the overall power balance, is a first step in the validation of the approach. However, this result does not allow for the derivation of statements considering local phenomena. In a next step, various input power values are compared with each other. The input power calculated from the divergence

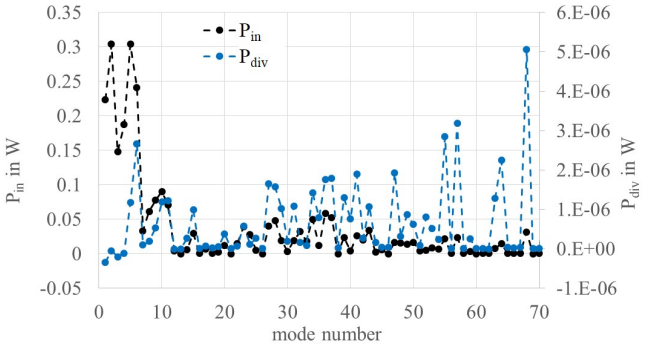

Figure 4: Comparison of the input power originating from the force excitation and the overall value for the integration of the STI's divergence over the whole surface of the plate

is estimated by summation of all positive power values in an area of twenty times twenty mm^2 with the excitation point in its center. The result is shown in Figure 5. Both curves show the same curve progression behaviour. Nonetheless, it can be seen that the divergence power value slightly overestimates the input power. This results from derivations through the approach that is used to get the necessary STI values for the numerical derivation. In Figures 1 and 3, the area of the force excitation shows increased negative values in the vicinity of the excitation point. By taking these values into account, the power balance of both values converge. This hints at a behaviour of the approach resulting in both increased positive and negative values in particular elements. However, this mistake corrects itself if the power balances are calculated over a wider area and needs to be examined in further analyses.

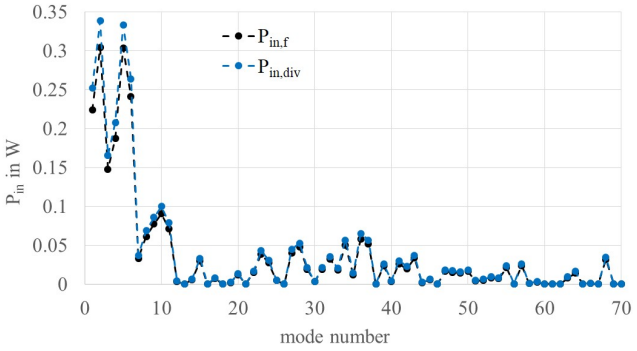

Figure 5: Comparison of the input power calculated from the force and through summation of all positive power values derived by the divergence in the vicinity of the force excitation of the test structure

A similar behaviour can be seen if the dissipated power values outside the area of the excitation are analysed. The dissipated power values gained through the values of the STI's divergence are compared with power values whose calculation basis is the strain energy density, e_{p}. Pavić shows that the real part of the STI's divergence has a relation to the strain energy density and the structural loss factor, η, at a specific angular frequency, Ω, in

the source-free field of the vibration [4]

$$\mathrm{Re}\left(\mathrm{div}\left(\underline{\mathbf{I}}_{\mathrm{s}}(f)\right)\right) = -2\eta\Omega e_{\mathrm{p}}. \tag{15}$$

Figure 6 shows the result for the calculated dissipated power of the various approaches. The curve progression is in all cases in accordance with the input power curve. The power values calculated from the strain energy density are considered as benchmark for the comparison because their values are in accordance with the input power calculated from the force. If the dissipated power, P_{div}, is calculated by summation of all negative values in the plate, it can be seen that the values differ for some of the eigenmodes of the structure. These differences disappear when the positive power values are taken into account for the balance, $P_{\mathrm{div,var}}$.

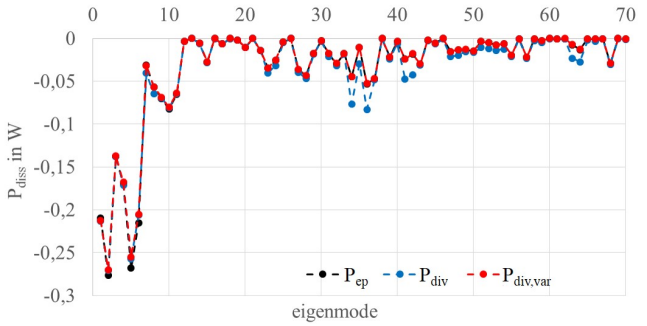

Figure 6: Comparison of the dissipated power estimated by various approaches

The reason for the discrepancy in the power values is again increased positive and negative values. The results for the numerical derivation of the respective modes show discrepancies. They possess positive divergence values in areas, where no energy input takes place. These pseudo sources lead to the difference in the calculated balance when they are neglected. If taken into account, the global balance is after all correct. The occurrence of these values needs to be taken into consideration by checking the plausibility of the results when one aims at describing local phenomena.

A last analysis is that of the behaviour of the divergence in context with the creation of the artificial connection area. The balances are calculated for the element sets directly connected to the auxiliary system boundaries. The graph in Figure 7 shows that the boundary on the left side of the connection is always identified as an energy sink. That means this is the boundary where the energy leaves the area under consideration. On the other hand, the boundary on the right side is always shown to be an energy source. Here, the energy enters the subsystem. This outcome is in accordance with the position of the force excitation on the lower left side of the plate. Both curves in the vicinity of the connection area exhibit the same curve progression and possess values with comparable magnitude. The outcome of the sum of both values is always negative since energy is dissipated in the connection area. In order to verify the significance of this result, further analyses will be conducted in the future.

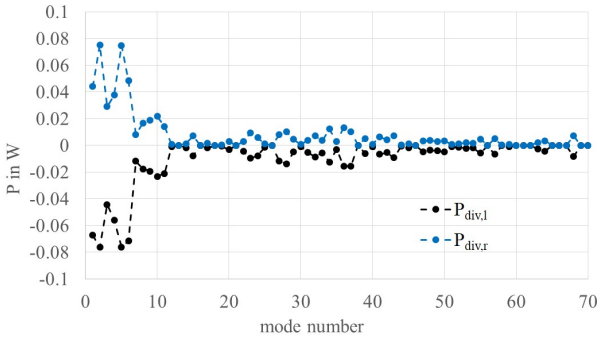

Figure 7: Power values at the element sets in the vicinity of the auxiliary boundaries

Summary and conclusions

In this paper, the idea of estimating and balancing power values in coupled subsystems by means of calculations based on the STI's divergence are introduced. It shows that the approach is able to identify energy sinks and sources and to give hints on the power balance in the system. A further goal that should be achieved with the introduced approach is that it should be possible to gain information on energy losses in rather complex connection structures such as hydraulic bearings, etc., by comparing the power balances of the thin-walled structures connected by them. The approach is able to give an idea about the order of the power loss in the connection element. The question on how reliable these results are must be clarified in further analyses.

In future studies more complex systems with more than one connection and more than one element type will be examined. In addition, the analysis will be extended to systems with fluid-structure interaction. This should yield further information on energy exchange processes between structures and fluids.

References

[1] Hering, T.: Strukturintensitätsanalyse als Werkzeug der Maschinenakustik. PhD thesis, Technische Universität Darmstadt, 2012

[2] Ebert, J.; Stoewer, T.; Schaal, C.; Bös, J.; Melz, T.: Opportunities and limitations on vibro-acoustic design of vehicle structures by means of energy flow-based numerical simulations. Proceedings of NOVEM 2015 Noise and Vibration – Emerging Technologies, Dubrovnik, Croatia, April 12–15, 2015, pp. 49798-1–49798-16

[3] Groba, P.; Ebert, J.; Stoewer, T.; Schaal, C.; Bös, J.; Melz, T.: Detection of energy sinks and sources in the active vibratory energy field of coupled structures and systems with fluid-structure interaction. Proceedings of ISMA2016 including USD2016, Leuven, Belgium, September 19–21, 2016, pp. 3945–3956

[4] Pavič, G.: The role of damping on energy and power in vibrating systems. Journal of Sound and Vibration, Vol. 281 (2005), pp. 45–71